

REAL AND VIRTUAL PHOTON STRUCTURE

L. JÖNSSON

*Department of Physics, Lund University, Box 118,
221 00 Lund, Sweden*



The structure of real and virtual photons has been studied in electron-proton scattering processes producing di-jet events at HERA by the H1 and ZEUS collaborations. Data have been compared to next-to-leading order QCD calculations and to the predictions of Monte Carlo generators based on the DGLAP and CCFM formalisms for describing the parton dynamics.

1 Introduction

Electron-proton scattering proceeds via the exchange of a virtual photon. For low values of the photon virtuality i.e. Q^2 close to zero we are in the region of photoproduction and as the virtuality increases above $Q^2 \sim 1 \text{ GeV}^2$ we enter the region of deep inelastic scattering (DIS). Electron-proton scattering events, which contain jets of high transverse momenta can be used to probe the partonic structure of either the proton or the exchanged photon, depending on the kinematic situation. As long as the transverse momentum of the parton propagator entering the hard scattering process is larger than the virtuality of the photon we will probe the constituents of the photon. This is obviously always true in photoproduction of high- p_t jets but may also be the case in DIS. Thus, comparisons with predictions of NLO perturbative QCD calculations and of Monte Carlo models will provide information about the structure of real as well as virtual photons.

We can distinguish between two classes of events where in one class the photon interacts as a pointlike particle (so called direct processes) and in the other the photon interacts via its partonic constituents (resolved photon processes). In the BFKL¹ description of the parton dynamics both these situations are taken into account in a natural way due to the arbitrary ordering of transverse momenta in the initial state parton ladder.

Experimentally the scaled photon energy, x_γ , is sensitive to the momenta of the incoming partons and can be used to separate direct photon processes from resolved ones. x_γ -spectra

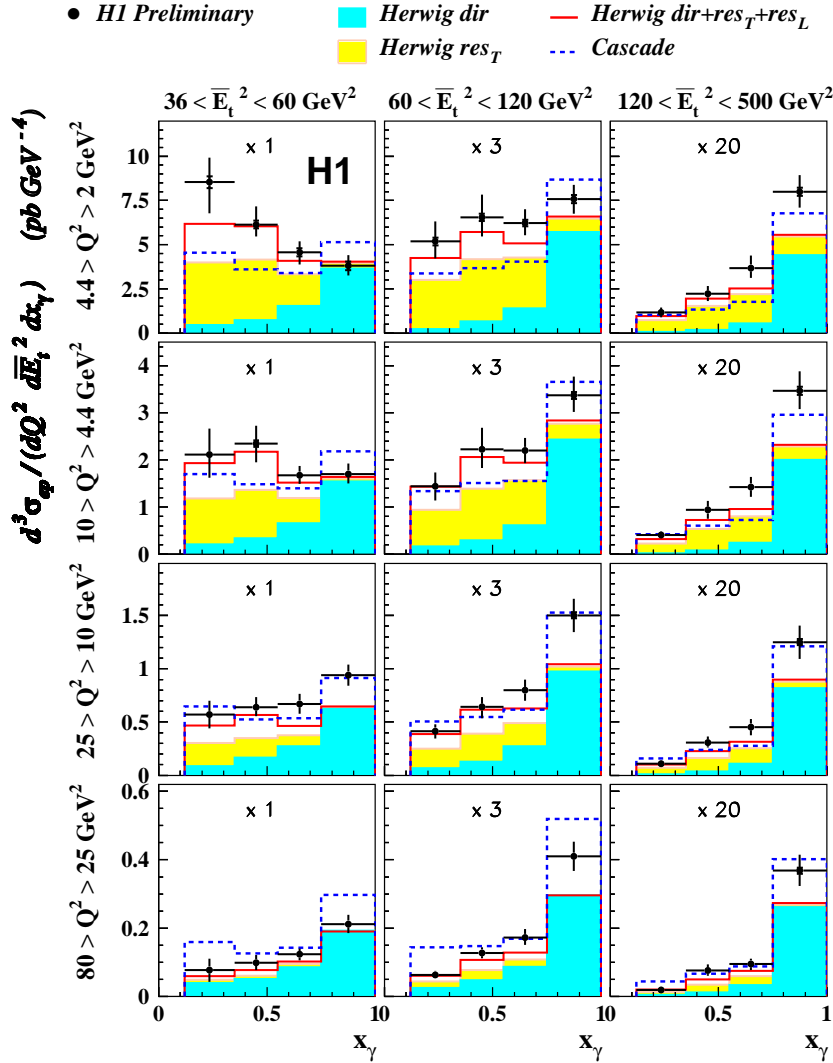


Figure 1: Triple differential cross section as a function of x_γ in bins of Q^2 and E_t^2 . Data are compared to the predictions of the HERWIG and CASCADE Monte Carlo generators.

from H1 and ZEUS show that a cut at around 0.7-0.8 gives a good separation between these classes of events.

2 The virtual photon structure

The virtual photon structure has been investigated by the H1 and ZEUS-collaborations in terms of triple differential di-jet cross sections, $d^3\sigma/dQ^2 dx_\gamma dy$.

Fig.1 shows results, obtained by the H1-experiment, on $d\sigma/dx_\gamma$ in bins of Q^2 and the transverse jet energy squared, E_t^2 . The data are compared to predictions from the HERWIG Monte Carlo program² assuming direct processes only (dark shaded histogram), direct plus resolved processes (light shaded histogram)³, and with the contribution of longitudinally polarised photons added (full line histogram)⁴. In addition the prediction of the CASCADE Monte Carlo program⁵ is given (broken line histogram). CASCADE is based on the CCFM formalism⁶, which in a consistent way implements the DGLAP⁷ and BFKL evolution equations. The figure

clearly shows that direct processes alone do not describe the data although the agreement is improved as Q^2 increases with respect to E_t^2 . The addition of resolved processes improves the situation over the whole kinematic range and even more so if the contribution from longitudinally polarised photons is taken into consideration. CASCADE with less degrees of freedom offers a description of the data which is of a similar quality as HERWIG including all photon contributions.

3 The real photon structure

The structure of real photons has been investigated by measuring the di-jet cross section in photoproduction at high transverse energies where a comparison with next-to-leading order (NLO) calculations is expected to be valid. In the measured kinematic domain non-perturbative effects like multiple interactions and hadronisation have been found to be small. The NLO calculation is based on the subtraction method⁸ in order to handle divergencies from collinear and infra-red emissions. Different parametrisations of the parton densities of the proton (CTEQ5M1⁹, MRST99¹⁰) and the photon (GRV-HO¹¹, AFG-HO¹²) were used to investigate the dependence of the NLO cross section to the parton density functions.

The H1 collaboration observes good agreement, over the full kinematic region investigated, between data and the NLO calculations with little dependence on the photon structure functions.

The ZEUS collaboration, on the other hand, finds that none of the photon structure functions used in the NLO calculations is able to give a fully satisfactory description of the data. Especially in kinematic regions where the photon structure function is expected to have a big influence, deviations between data and NLO calculations are observed. This would indicate that higher order corrections are important. It should however be noted that the dominant theoretical uncertainty, coming from variations in the renormalisation and factorisation scales, completely account for the observed deviations. Thus further constraints of the density functions require a better theoretical understanding of the scale dependence.

4 Di-jet production associated with charm

As has already been observed in Fig.1, measurements have clearly shown that the influence of the partonic structure of the photon decreases as its virtuality increases. The ZEUS collaboration has studied the cross section ratio of direct and resolved photon processes for di-jet events containing a D^* -meson. Data have been compared to predictions of the HERWIG Monte Carlo program using two options of the SAS1D parametrisation for the virtual photon. One option considers a suppression of the partonic structure with increased photon virtuality, whereas the other does not.

From Fig.2a it is evident that the present data do not have the necessary precision to be sensitive to a possible Q^2 -suppression as given by SAS1D. However, the absence of an overall Q^2 -dependence of the cross section ratio in this data stays in sharp contrast to what has been observed for di-jet events without any charm requirement. This fact indicates that the suppression at low x_γ due to the charm requirement and due to the virtuality are not independent. Fig.2b gives a comparison of data with two models, which do not include any partonic structure of the photon. The AROMA model¹³ is based on the conventional DGLAP evolution scheme, whereas the CASCADE model uses the CCFM evolution equations. The data clearly favour the CCFM based description with non k_t -ordered parton emissions in the initial state. The ratio of di-jet events containing a D^* -meson in one of the jets is shown in Fig.2c and compared to what is expected from the description of SAS1D including all flavours but not requiring any D^* -meson. The SAS1D prediction shows a clear Q^2 -suppression inconsistent with data. However, it was found that the kinematic cuts applied to select D^* -mesons cause a suppression of the resolved

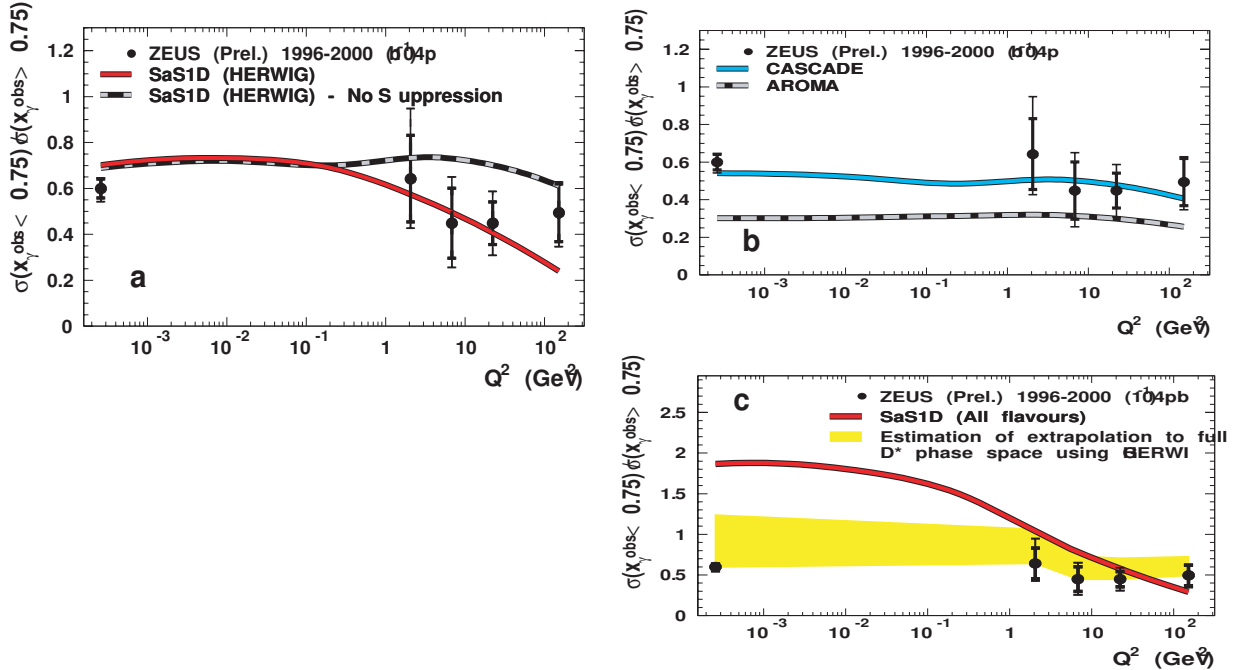


Figure 2: Ratio of low to high x_γ for di-jet events with a D^* meson. Data are compared to (a) the predictions of the SAS1D photon structure function, (b) the AROMA and CASCADE Monte Carlo programs and (c) the SAS1D photon structure function without the requirement of a D^* .

contribution. The HERWIG Monte Carlo program was used to extrapolate the cross section ratio to the full phase space for D^* -production. This is given by the shaded band in the figure and is consistent with no Q^2 -suppression in contrast to what is expected if no charm is required.

Photoproduction of charm is an ideal testing ground for studying the underlying parton dynamics, since charm is predominantly produced by $\gamma \rightarrow c\bar{c}$. The observation of an emission (jet) with $p_t > p_t^c(p_t^{\bar{c}})$ indicates a scenario which is possible in DGLAP only in a full $O(\alpha_S^2)$ calculation or when charm excitation of the photon is included (the resolved photon case). However, in the BFKL description such a scenario comes naturally, since the transverse momenta along the evolution chain are not ordered. The measured x_γ spectrum shows a tail to small values, indicating that the hardest emission is indeed not always coming from the charm quarks. Simulations with the CASCADE generator shows that a significant part of the cross section comes from events, where the gluon is the jet with the largest transverse momentum. A comparison of the measurement from the ZEUS collaboration with the prediction from the full event simulation of CASCADE using the unintegrated gluon distribution as given by Jung and Salam¹⁴ and applying jet reconstruction and jet selection at the hadron level shows reasonably good agreement¹⁵.

5 Conclusions

Studies of the real and virtual photon structure have clearly shown that NLO calculation and Monte Carlo generators using the DGLAP evolution scheme are able to give reasonable agreement with data only if contributions from resolved photon processes are included. On the other hand, the CASCADE Monte Carlo program, in which the CCFM evolution equations are implemented, gives an equally good description of the data but with less free parameters.

Acknowledgments

I have profited from helpful discussion with M. Derrick, E. Elsen, H. Jung and P. Schleper. The Swedish Research Council is acknowledged for financial support.

References

1. E. Kuraev, L. Lipatov, V. Fadin, *Sov.Phys JETP* **44**, 443 (1976)
E. Kuraev, L. Lipatov, V. Fadin, *Sov.Phys JETP* **45**, 199 (1977)
Y. Balitskii, L. Lipatov, *Sov.J.Nucl.Phys.* **28**, 822 (1978).
2. G. Marchesini *et al*, *Comp.Phys.Comm.* **67**, 465 (1992).
3. H. Jung, L. Jönsson, H. Küster, *Eur.Phys.J. C* **9**, 383 (1999).
4. J. Chyla, *Phys. Lett. B* **488**, 289 (2000)
5. H. Jung, in *Workshop on Monte Carlo generators for HERA*, ed. A. Doyle, G. Grindhammer, G. Ingelman, H. Jung, hep-ph/9908497
H. Jung, *Comp.Phys.Comm.* **143**, 100 (2002).
6. M. Ciafaloni, *Nucl. Phys. B* **296**, 49 (1988)
S. Catani, F. Fiorani, G. Marchesini, *Phys. Lett. B* **234**, 339 (1990)
S. Catani, F. Fiorani, G. Marchesini, *Nucl. Phys. B* **336**, 18 (1990)
G. Marchesini, *Nucl. Phys. B* **445**, 49 (1995).
7. V. Gribov, L. Lipatov, *Sov.J.Nucl.Phys.* **15**, 438 and 675 (1972)
L. Lipatov, *Sov.J.Nucl.Phys.* **20**, 94 (1975)
G. Altarelli, G. Parisi, *Nucl. Phys. B* **126**, 298 (1977)
Y. Dokshitzer, *Sov.Phys JETP* **46**, 641 (1977).
8. S. Frixione, Z. Kunszt, A. Signer, *Nucl. Phys. B* **467**, 399 (1996)
S. Frixione, *Nucl. Phys. B* **507**, 295 (1997)
S. Frixione and G. Ridolfi, *Nucl. Phys. B* **507**, 315 (1997).
9. H.L. Lai *et al*, *Phys. Rev. D* **55**, 1280 (1997).
10. A.D. Martin, R.G. Roberts, W.J. Stirling, R.S. Thorne, *Eur.Phys.J. C* **C14**, 133 (2000).
11. M. Glück, E. Reya, A. Vogt, *Phys. Rev. D* **45**, 3986 (1992)
M. Glück, E. Reya, A. Vogt, *Phys. Rev. D* **46**, 1973 (1992).
12. P. Aurenche, J. Guillet, M. Fontannaz, *Z. Phys. C* **64**, 135 (1997).
13. G. Ingelman, J. Rathsman, G.A. Schuler, *Comp.Phys.Comm.* **101**, 465 (1992).
14. H. Jung and G. Salam, *Eur.Phys.J. C* **19**, 351 (2001).
15. S.P. Baranov, H. Jung, L. Jönsson, S. Padhi, N.P. Zotov, *Eur.Phys.J. C* DOI **10.1007/s10052-002-0957-3**, (2002).